

# Magnetic properties of the polycrystalline $\text{Cu}_x\text{FeCr}_{1-x}\text{O}_2$ in low field

BERDAN OZKURT\*, OSMAN MURAT OZKENDİR

*Mersin University, Tarsus Faculty of Technology, Dept. of Energy Systems Engineering, Tarsus, Turkey*

Electronic and magnetic properties of the polycrystalline samples with the general formula  $\text{Cu}_x\text{FeCr}_{1-x}\text{O}_2$  (where  $0 < x < 1$ ) have been studied by various techniques. The effects of  $\text{Cr}^{3+}$  substitution on the magnetic properties of  $\text{CuFeO}_2$ , as a starting material, were examined by hysteresis measurements. Magnetic studies of the samples were also supported by Magnetic Circular Dichroism measurements. All the samples were determined as showing a magnetic transition peak at characteristic Néel Temperature ( $T_N$ ) temperature from antiferromagnetic to paramagnetic ordering. Besides, the effect of high external magnetic field ( $H > 2T$ ) to magnetic ordering were also studied and a change from paramagnetic to AFM at high magnetic fields observed. However, according to the decreasing Cu concentration in the sample, prominent changes both in intensity and in the anti-ferromagnetic ordering structure determined.

(Received February 28, 2013; accepted March 13, 2014)

*Keywords:* Hysteresis, Circular dichroism, Magnetism, Magnetic materials

## 1. Introduction

In the last decade, ferromagnetic materials became one of the major field in technological applications. Besides, semiconductor properties, eminent magnetic properties and possible huge magneto-electric effects make them highly favorable field of study in science. One of the leading and the most popular magnetic member of 3d transition metal group is the "iron". Although iron is a ferromagnetic material, most of the iron oxides show anti-ferromagnetic properties, like;  $\text{Fe}_2\text{O}_3$  and  $\text{CuFeO}_2$ .

$\text{CuFeO}_2$  is a member of both antiferromagnetic iron oxides and the delafossite-type "ABO<sub>2</sub>" compounds with two reported Néel Temperatures ( $T_N$ ) at 10.5K and 14K, respectively. Delafossite-type ABO<sub>2</sub> compounds, where "A =  $\text{Cu}^{1+}$ ,  $\text{Ag}^{+1}$ " and "B =  $\text{Fe}^{3+}$ ,  $\text{Cr}^{3+}$ ,  $\text{Al}^{3+}$ " have been extensively studied because of their many interesting physical properties [1,2,8]. In delafossite  $\text{CuFeO}_2$  structure, triangular lattices of  $\text{Fe}^{3+}$  layers are separated by nonmagnetic  $\text{Cu}^{+1}$  and  $\text{O}^{-2}$  layers [3,4]. This formation is one of the reasons of antiferromagnetic ordering in the structure. Also, oxygen non-stoichiometry largely affects the anti-ferromagnetism of delafossite  $\text{CuFeO}_2$  crystal [5]. Besides, in ABO<sub>2</sub> structures, Cu-Cu interatomic interactions are responsible for very high electrical conductivity. Additionally,  $\text{CuFeO}_2$  is known as a *p*-type semiconductor with the band gap of 1.15eV [2, 6, 7].

Magnetic studies for these systems are extremely important because of interesting electromagnetic interactions between electron's spin and the magnetic effect produced by the orbital motion of its adjacent electrons. On the other hand, the interaction between localized magnetic moment and carriers can effect band structure and behavior of carriers. The magnetic behavior of the structure significantly change the effect of

substitution elements which had magnetic effects on the structure of delafossite-type compounds. Such substitutions can change both the remanent magnetization ( $M_r$ ) and coercive ( $H_c$ ) properties of the structure effectively, which are considered as an extrinsic property of the material.

Absorption spectroscopy techniques are the best tools to probe the electronic and magnetic structures of materials. The magnetic properties of 3d transition metals are best reflected by their *d* valence electrons. According to study on the magnetic properties of transition metals and their oxides by absorption processes, core electrons, i.e., K and L-edge electrons, are excited to unoccupied valence levels as a final state above the Fermi level. In this process, core hole magnetic moments interact with 3d level unoccupied states (holes) and cause strong coupling which can be best investigated by X-ray Magnetic Circular Dichroism (XMCD) method. XMCD is a very sensitive method both in magnetic moments (even very small magnetic moments) and structural environment of the material, where the XMCD spectra are derived from two different measurement data which are collected by the coupling of two different x-rays (parallel and anti-parallel helicities) with the electron spins of the sample.

The main purpose of this study is to investigate the effects of Cr doping in  $\text{CuFeO}_2$  structure on magnetic structure via magnetic and electronic behaviors. As known from the previous studies, in ABO<sub>2</sub> type compounds, Cr ions tend to sit in the Fe locations and construct the structure from  $\text{CuFeO}_2$  to  $\text{CuCrO}_2$  [8,9]. However, in the present work, the substitution effects of Chromium on the magnetic behavior of  $\text{Cu}_x\text{FeCr}_{1-x}\text{O}_2$  samples at very low and room temperatures while changing Cu concentration (decrease) with Cr concentration (increase) in the structure were investigated.

## 2. Experimental details

Polycrystalline  $\text{Cu}_x\text{FeCr}_{1-x}\text{O}_2$  samples were synthesized by conventional solid state reaction method with stoichiometric mixtures of  $\alpha\text{-Fe}_2\text{O}_3$  (Hematite),  $\text{CrO}_3$  and  $\text{CuO}$  powder compounds as starting materials with high purity (>99.99%). The starting powder  $\text{CrO}_3$  is known to form  $\text{Cr}_2\text{O}_3$  at an annealing process over  $197^\circ\text{C}$ . The powders were mixed in stoichiometric ratios according to changes in concentration by “ $x$ ”. Mixed powders were grinded for 1h and calcined in air at  $550^\circ\text{C}$  for 5 hours. After annealing process, mixed powders regrinded for 1h and sintered in air at  $950^\circ\text{C}$  for 24 h.

The XRD patterns of  $\text{CuFeO}_2$ ,  $\text{Cu}_{0.8}\text{FeCr}_{0.2}\text{O}_2$  and  $\text{Cu}_{0.4}\text{FeCr}_{0.6}\text{O}_2$  (i.e. for  $x=1, 0.8, 0.4$ ) structures are given in Fig. 1. These three structures are presented in the same figure for comparison of the “ $x$ ” dependence. Different formations, other than  $\text{CuFeO}_2$  structures, are highlighted with different letters, as a guide for eyes. Apparently, due to the decreasing Cu and increasing Cr concentrations in the structure, Cr atoms tend to form  $\text{CrO}_2$  and  $\text{Cr}_2\text{O}_3$  clusters. However, the  $\text{CrO}_2$  formations have higher intensity in low “ $x$ ” values. The Cu presence in the bulk decreases the possibility of  $\text{Cr}_2\text{O}_3$  formation in the structure. These new formations according to the values of  $x$  in the structure, affects the Fe environment via Cr-O bonding and  $d-d$  interaction between Fe and Cr. It is clear that, the change in the environment of an atom cause changes both in electronic and magnetic structure.

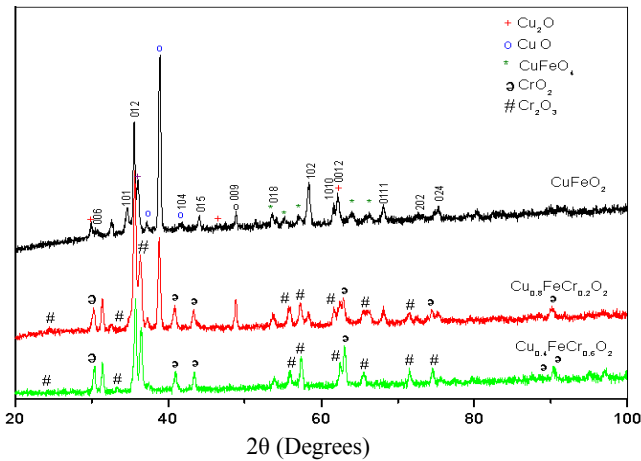


Fig. 1. XRD Pattern of  $\text{Cu}_x\text{FeCr}_{1-x}\text{O}_2$  structure for  $x=1, 0.8, 0.4$ .

The magnetic measurements of the compound were performed with a 7304 model Lake Shore VSM after cooling the sample in zero magnetic field (ZFC), from room temperature to low temperatures at  $\pm 10$  kOe.

Additionally, the magnetic properties of  $\text{Cu}_x\text{FeCr}_{1-x}\text{O}_2$  polycrystals are measured by x-ray magnetic circular dichroism technique under 3 Tesla external magnetic field. The Fe L-edge measurements are performed at IMS, UVSOR-II Synchrotron Facility (Okazaki, Japan), at the beamline BL4B at low temperature (5 K) and Ultra High

Vacuum (UHV) conditions ( $\sim 10^{-10}$  Torr). The XMCD measurement system obtains polarization by a split superconducting magnet with a maximum magnetic field of 7 T. The XMCD spectra were recorded with a total electron yield mode by detecting a drain current from the sample.

## 3. Results and discussion

To probe the effects of Cr substitution on the electronic structure of  $\text{Cu}_x\text{FeCr}_{1-x}\text{O}_2$  samples, X-ray absorption Near-edge Structure (XANES) spectroscopy measurements are performed as the first step.

In the Fig. 2, Fe  $L_{3,2}$ -edge XANES spectra of  $\text{CuFeO}_2$  are compared with the spectra of  $\text{Cu}_x\text{FeCr}_{1-x}\text{O}_2$  samples with  $x$  values as; 0.8, 0.6, 0.4 and 0.2. Fe  $L_3$ -edge absorption spectrum of  $\text{CuFeO}_2$  begins to rise at 706.9 eV and have a maximum at 711.3 eV, while Fe  $L_2$  absorption edge begins to rise at 720.3 eV and have a maximum at 723.8 eV. The  $L_3$  and  $L_2$  edge energies correspond to the  $2p_{3/2}$  and  $2p_{(1/2)}$  electrons transition to unoccupied  $3d$  levels as a final state, respectively.

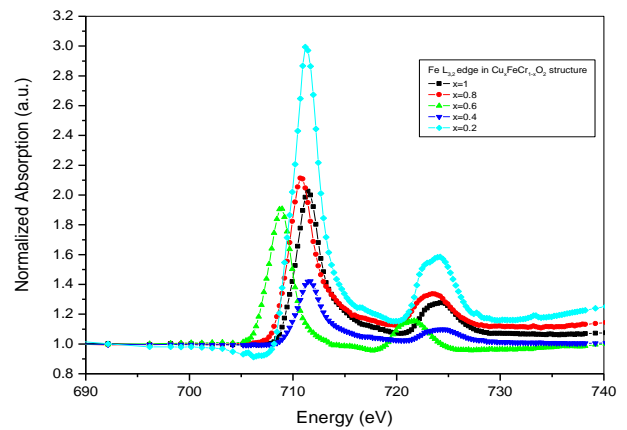


Fig. 2. XANES spectra of the  $\text{Cu}_x\text{FeCr}_{1-x}\text{O}_2$  samples.

As seen in the figure, the spectra for  $x=1$  sample has a “so weak” shoulder-like pre-edge structure. Delafossite  $\text{CuFeO}_2$  is an antiferromagnetic iron oxide with space group ( $R\bar{3}m$ ) forms in the triangular structure with hexagonal layers of distorted  $O_h$  symmetry, like  $\alpha\text{-Fe}_2\text{O}_3$  [2-5]. The “weak” curve in the pre-edge reflects the different symmetry rather than  $O_h$  in the structure which can be best analyzed by XMCD measurements.

Among all sample spectra, an energy shift appears to low energy side with the Cr substitutions in the structure; slightly for  $x=0.8$  and strongly for 0.6, according to the electronic structure of  $\text{CuFeO}_2$  ( $x=0$ ) as a reference. These shifts highlight the presence of local crystal formations with higher symmetry than delafossite structure which provides available low energy levels as a final state in absorption process; i.e. broader molecular bands. Besides, the shift is also a sign of disturbance in crystal fields. The measured shifts at the absorption energies of  $x=0.8$  and 0.6 values are 0.7 and 2.7 eV, respectively.

The system has delafossite structure and new Cr dopants can only sit in the Fe places in the  $ABO_2$  structures. However, the number of Fe atoms was kept constant, unlike with copper. This is a chaos in the structure forcing the system to a phase transition where Cr and Fe can occupy individual locations. The phase transitions in the structure seem to happen between  $x=0.6-0.4$  values. The higher energy shift ( $\sim 2.7$  eV) at  $x=0.6$  with a decrease in the intensity is an evidence for the phase transformation reflecting higher quantum symmetries. The structural transformation almost seems to have finished at  $x=0.4$ . This is proved by the disappearance of the energy shift due to instabilities in the crystal. Besides, the lower intensity is a result of weak effect of new structure construction. However, the highest intensity at  $x=0.2$  is a result of strongly overlapped Fe bonds with neighboring O and especially Cr ions in the new phase, where strong  $d-d$  interaction takes place.

To support the study both on the crystal structure and the magnetic ordering properties in  $Cu_xFeCr_{1-x}O_2$  samples, XMCD measurements are performed and given in Fig. 3, in comparison with all  $x=1, 0.8, 0.6, 0.4$  and  $0.2$  values.

During the ferromagnetic ordering in a material, atomic magnetic moments are oriented parallel to external magnetic field ( $\mathbf{H}$ ) because of the spin orbit coupling and give negative spectra for  $L_3$ . For the same situation  $L_2$ -edge spectra have almost positive MCD signals [10]. These basic definitions are the mainlines for determining the magnetic structure by measured XMCD spectra of the samples.

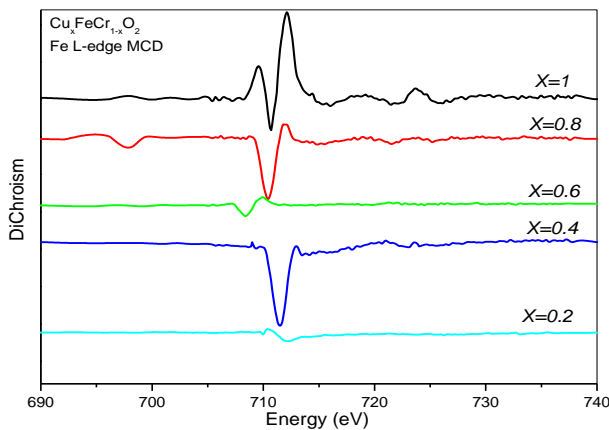


Fig. 3. XMCD spectra of the  $Cu_xFeCr_{1-x}O_2$  samples.

For  $x=1$  value, the “ $CuFeO_2$ ” structure,  $L_3$ -edge spectrum has two positive peaks and a negative peak, however, the  $L_2$ -edge spectrum has only a positive peak. Different orientation of the peaks in the spectra confirms the anti-ferromagnetic interaction between  $Fe^{+3}$  layers which are separated by Cu-O layers in structure [3,4]. Besides, the anti-parallel oriented regions in the structure reflects the local symmetry  $O_h$  of the main clusters.

However, the parallel oriented region, at the “so weak” pre-edge of  $L_3$  spectrum, is due to the  $T_d$  local symmetry sites.  $T_d$  sites couple with the  $\mathbf{H}$  ferromagnetically. This coupling points out the formation of  $\gamma-Fe_2O_3$  (maghemite) in the structure which is a ferrimagnetic member of the iron (III) oxides with local  $T_d$  site symmetry [11].

Apparently, the anti-ferromagnetic structure becomes weaker with decreasing Cu concentration in the sample. For  $x=0.8$ , one of the positive signal part of the spectrum vanished while the negative spectrum part is getting stronger. Cr substitutions in the structure cause structural deformation in some parts of the crystal domains and weakens the reasons of anti-ferromagnetic ordering. The traces of structural deformation are apparent at  $x=0.6$  concentration by a shift about 2 eV to lower energy side. However, for  $x=0.4$ , the spectral intensity and characteristics are similar to  $x=0.8$  concentration, but give some clues about ferromagnetic ordering under higher external magnetic field. As given in Figure 1, due to the increasing ferromagnetic  $CrO_2$  formations in the structure, ferromagnetic ordering which is originated by  $Fe^{+3}$  ions are supported.

In order to understand the magnetic characteristics of the samples, the magnetic properties of  $Cu_xFeCr_{1-x}O_2$  were determined from hysteresis measurements. The Figs. 4 and 5 shows the magnetization hysteresis curves measured at various temperatures for all samples. It is clearly seen from the figures that the saturation magnetization and hysteresis  $H_C$  strongly depend on the doped element in the material. At  $T=300K$ , the value of  $H_C$  and  $M_S$  decreases significantly due to the randomly distributed magnetic moments in the high temperature range, as expected. Another reason of these decreases is the spin canting effect which occurs when ordered magnetic moments are deflected from their plane. The substitutions of  $Cr^{3+}$  cations into the structure causes a different change in the values of net magnetism. The magnetization values become narrower with the increasing temperature.

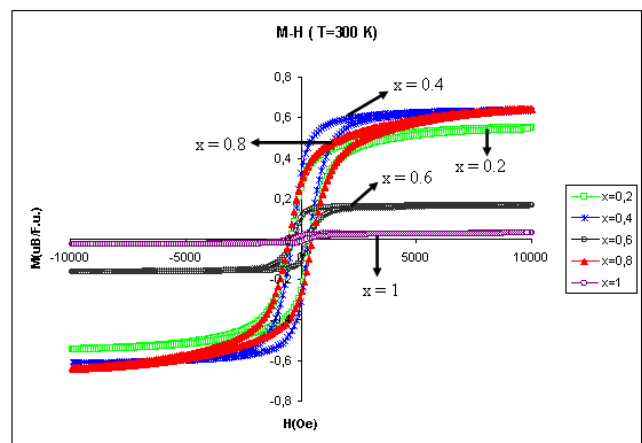


Fig. 4. Magnetization hysteresis curves measured at 300 K.

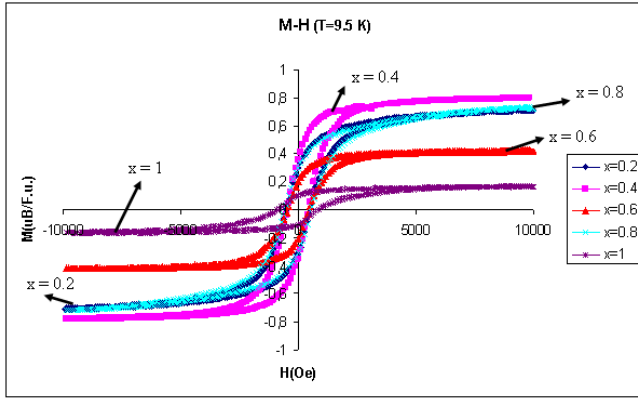


Fig. 5. Magnetization hysteresis curves measured at 9.5 K.

Table 1. Magnetizations, coercive forces ( $H_C$ ), and ratios of remanent induction to saturation magnetization ( $M_r/M_S$ ), for the  $\text{CuFeO}_2$  samples prepared in various concentration.

		x = 0.2	x = 0.4	x = 0.6	x = 0.8	x = 1
9.5 K	$M_S$ (emu/gr)	26,442	30,35	16,04	28,49	6,66
	$H_C$ (G)	493,75	460	453,74	558	863
	$M_r/M_S$	0,439	0,449	0,523	0,437	0,642
300 K	$M_S$ (emu/gr)	20,67	24,228*	6,473	25,276	1,1866
	$H_C$ (G)	439,5	385*	335	509	369
	$M_r/M_S$	0,454	0,495*	0,579	0,419	0,547

\* It is made at 200 K.

The  $M_r/M_S$  values of the samples were studied both at 9K and 300K. The low values which are given in the Table 1, can also be interpreted as weak interactions among particles with uniaxial anisotropy. Ordinarily, the unstable values of the saturation moment  $M_S$ , which is an intrinsic property of the material, reflect the anti-parallel alignment of some ferromagnetic domains through the anti-ferromagnetic region, depending on the amount of the doped element.

In the Fig. 6, both  $M_{ZFC}$  and  $M_{FC}$  data measured with  $H = 1\text{kOe}$  as a function of temperature are given. Below the  $T_N$  temperature, each of the samples show irreversibility between the ZFC-magnetization ( $M_{ZFC}$ ) and the FC-magnetization ( $M_{FC}$ ). However,  $M_{ZFC}$  and  $M_{FC}$  coincide with each other at high temperatures. As the temperature decreases, both  $M_{ZFC}$  and  $M_{FC}$  increase monotonously. All the samples show a peak of magnetic transition. The field cooled data have a distinction from zero field cooled data around the peak temperature. On the other hand, it is generally expressed that the difference between  $M_{ZFC}$  and  $M_{FC}$  is a spin glass like state below about  $T_N$  [13,14].

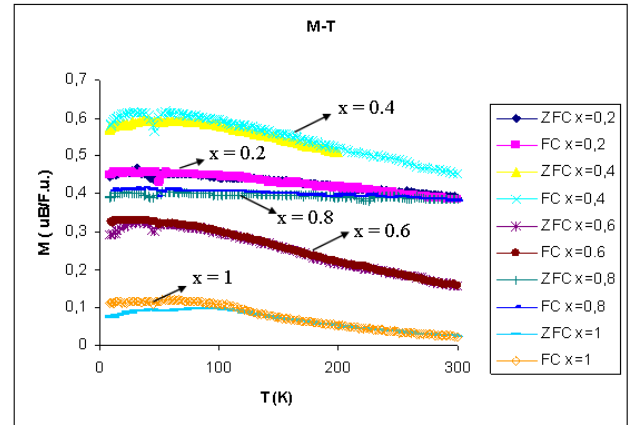


Fig. 6. Magnetizations in zero field cooled (ZFC) and field cooled (FC) conditions under applied field of 1kOe as a function of temperature.

In Table 1, the saturation magnetization, the coercive force, and the ratio of remanent induction to saturation magnetization are listed. Apparently, the saturation magnetizations are considerably influenced by the change of  $x$  values. An isotropic behavior is observed where the distribution of the magnetic orientations in the grains is uniform for all samples. This is due to the value of  $M_r$  for an isotropic magnet, i.e. is equal about to  $0,5M_S$ . It is well known that the coercivity is intimately connected with the total anisotropy via the relation grain boundaries [12-14].

In the Fig. 7, the magnetization measurements of the samples are shown which suits best to the definition given in the previous paragraph. The value of magnetizations below  $T_N$  are higher than in zero-field cooling and describes also the existence of some magnetic short-range order. There are visible peaks at  $T_N$  temperatures, at which the magnetic ordering of all samples change from ferromagnetic to anti-ferromagnetic ordering.

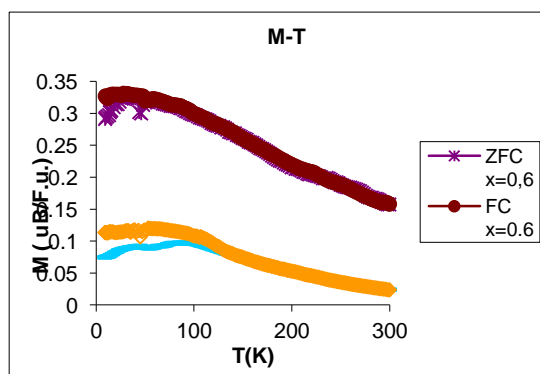


Fig. 7. Magnetization versus temperature curves in a field of 10 kOe for  $x = 0,6$  and 1.

In Fig. 8, the change of the Néel temperature with the increase of dopant concentration is presented. In the case of Cr substitution, the change in the  $T_N$  temperature is not linear. According to the measurements, the highest value of Néel point was measured for  $x = 1$ .

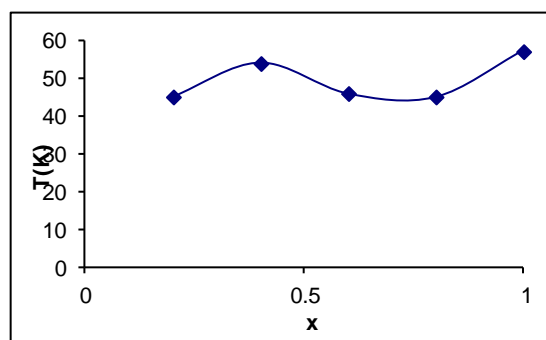


Fig. 8. Concentration ( $x$ ) dependence of Néel temperature  $T_N$ .

#### 4. Conclusions

In this study, the magnetic and electronic structure of delafossite  $\text{Cu}_x\text{FeCr}_{1-x}\text{O}_2$  oxides are investigated via increasing Cr substitution versus Copper, according to the formula where  $x$  has value as 0.2, 0.4, 0.6, 0.8 and 1, respectively. The effect of partial  $\text{Cr}^{3+}$  substitution on the magnetic properties of  $\text{CuFeO}_2$  were examined while decreasing Cu concentrations by magnetic and XMCD measurements.

For low temperature values, anti-ferromagnetic (AFM) ordering for all structure is observed. However, at 300 K temperature,  $\text{CuFeO}_2$  seem to have no anti-ferromagnetic ordering, but the rest of the samples have AFM ordering in the structure. This magnetic behavior is a result of ferromagnetic  $\text{CrO}_2$  and antiferromagnetic  $\text{Cr}_2\text{O}_3$  oxide formations in the structures. It was reported in previous studies that; Curie Temperature ( $T_c$ ) for ferromagnetic  $\text{CrO}_2$  and  $T_N$  for antiferromagnetic  $\text{Cr}_2\text{O}_3$  are; 390K and 307 K, respectively [15].

According to the decreasing Cu (increasing Cr) concentrations, structural transition with change in magnetic properties are determined. The change in the

spectra is thought to cause due to partial crystal structure transitions from delafossite structure to corundum structure where  $\text{Cr}_2\text{O}_3$  and  $\text{CrO}_2$  clusters appear other than  $\text{Cu}^{+1}$  and O blocks.

#### Acknowledgments

The authors would like to thank to Prof. Dr. Bekir OZCELIK from Cukurova University Physics Department and Prof. Dr. Nevzat KULCU from Mersin University Chemistry Department because of opening their laboratories to us. We also would like to thank Mr. Onur NANE, Dr. Tetsuya HAJIRI and Miss Tulay CETIN for their experimental support.

This study is partly supported by BIDEB-2219 grant of TUBITAK (Ankara, Turkey).

#### References

- [1] R. D. Shannon, C. T. Prewitt, D. B. Rogers, *Inorg. Chem.* **10**, 719 (1971).
- [2] B. V. Beznosikov, K. S. Aleksandrov, *Journal of Structural Chemistry.* **50**(1), 102 (2009).
- [3] H. Takahashi, Y. Motegi, R. Tsuchigane, M. Hasegawa, *J. of Magnetism and Magnetic Materials* **272-276**, 217 (2004).
- [4] O. M. Ozkendir, *J. Optoelectron. Adv. Mater. – Rapid Comm.* **3**(6), 586 (2009).
- [5] M. Hasegawa, M. I. Batrashevich, T. R. Zhao, H. Takei, *Mater. Res. Bull.* **32**, 151(2001).
- [6] *State Diagrams of High-Melting Oxide Systems: Handbook, Double Systems (issue 5)[in Russian]*, Part 3, Nauka, (1987) Leningrad.
- [7] Kei Hayashi, Tomohiro Nozaki, Tsuyoshi Kajitani, *Japanese Journal of Applied Physics*, **46**(8A), 5226 (2007).
- [8] O. Aktas, K. D. Truong, T. Otani, G. Balakrishnan, M. J. Clouter, T. Kimura, G. Quirion, *Journal of Physics-Condensed Matter* **24**, 036003 (2012).
- [9] P. T. Barton, R. Seshadri, A. Knoeller, M. Rosseinsky, *Journal of Physics-Condensed Matter* **24**, 016002 (2012).
- [10] S. Brice-Profeta, M. A. Arrio, E. Tronc, N. Menguy, I. Letard, C. Cartier dit Moulin, M. Nogues, C. Chaneac, J. P. Jolivet, Ph. Saintavit, *Journal of Magnetism and Magnetic Materials* **288**, 354 (2005).
- [11] L. X. Chen, T. Liu, M. C. Thurnauer, R. Csencsits, T. Rajh, *J. Phys. Chem. B* **106**, 8539 (2002).
- [12] H. Kronmüller, K. D. Durst, M. Sagawa, *J. Magn., Magn. Mater.*, **74**, 291(1988).
- [13] S. Radha, A. K. Nigam, S. K. Malik, Girish Chandra, *Journal of Magnetism and Magnetic Materials*, **140-144**, 101 (1995).
- [14] Y. Tazuke, *Journal of Magnetism and Magnetic Materials*, **140-144**, 155 (1995).
- [15] R. Cheng, A. N. Caruso, L. Yuan, S.-H. Liou, P. A. Dowben, *Applied Physics Letters* **82**, 354 (2003).

\*Corresponding author: berdanozkurt@mersin.edu.tr